



# Assessing the role of amino acids in systemic inflammation and organ failure in patients with ACLF

Giacomo Zaccherini<sup>1,2,†</sup>, Ferran Aguilar<sup>1,†</sup>, Paolo Caraceni<sup>2</sup>, Joan Clària<sup>1,3,4</sup>, Juan José Lozano<sup>4</sup>, François Fenaille<sup>5</sup>, Florence Castelli<sup>5</sup>, Christophe Junot<sup>5</sup>, Anna Curto<sup>1</sup>, Chiara Formentin<sup>6</sup>, Emmanuel Weiss<sup>1,7</sup>, Mauro Bernardi<sup>2</sup>, Rajiv Jalan<sup>1,8</sup>, Paolo Angeli<sup>1,6</sup>, Richard Moreau<sup>1,9,10,\*‡</sup>, Vicente Arroyo<sup>1,‡</sup>

<sup>1</sup>EF Clif, EASL-CLIF Consortium and Grifols Chair, Barcelona, Spain; <sup>2</sup>Department of Medical and Surgical Sciences, University of Bologna, Bologna, Italy; <sup>3</sup>Hospital Clínic-IDIBAPS, Universitat de Barcelona, Barcelona, Spain; <sup>4</sup>CIBERehd, Barcelona, Spain; <sup>5</sup>Service de Pharmacologie et Immuno-Analyse (SPI), Laboratoire d'Etude du Métabolisme des Médicaments, CEA, INRA, Université Paris Saclay, MetaboHUB, F-91191 Gif-sur-Yvette, France; <sup>6</sup>Unit of Internal Medicine and Hepatology, Dept. of Medicine, DIMED, University of Padova, Italy; <sup>7</sup>Assistance Publique – Hôpitaux de Paris (AP-HP), Department of Anesthesiology and Critical Care, Beaujon hospital, DMU Parabol, AP-HP Nord, Paris, France; <sup>8</sup>Liver Failure Group, Institute for Liver and Digestive Health, University College London, Royal Free Campus, London, United Kingdom; <sup>9</sup>Inserm, Université de Paris, Centre de Recherche sur l'Inflammation (CRI), Paris, France; <sup>10</sup>Assistance Publique – Hôpitaux de Paris, Service d'Hépatologie, Hôpital Beaujon, Clichy; France

See Editorial, pages 1015–1017

**Background & Aims:** Systemic inflammation and organ failure(s) are the hallmarks of acute-on-chronic liver failure (ACLF), yet their pathogenesis remains uncertain. Herein, we aimed to assess the role of amino acids in these processes in patients with ACLF.

**Methods:** The blood metabolomic database of the CANONIC study (comprising 137 metabolites, with 43% related to amino acids) – obtained in 181 patients with ACLF and 650 with acute decompensation without ACLF (AD) – was reanalyzed with a focus on amino acids, in particular 9 modules of co-regulated metabolites. We also compared blood metabolite levels between ACLF and AD.

**Results:** The main findings in ACLF were: i) Metabolite modules were increased in parallel with increased levels of markers of systemic inflammation and oxidative stress. ii) Seventy percent of proteinogenic amino acids were present and most were increased. iii) A metabolic network, comprising the amino acids aspartate, glutamate, the serine-glycine one-carbon metabolism (folate cycle), and methionine cycle, was activated, suggesting increased purine and pyrimidine nucleotide synthesis. iv) Cystathionine, L-cystine, glutamate and pyroglutamate, which are involved in the transsulfuration pathway (a methionine cycle branch) were increased, consistent with increased synthesis of the antioxidant glutathione. v) Intermediates of the catabolism of 5 out of the 6 ketogenic amino acids were increased. vi) The

levels of spermidine (a polyamine inducer of autophagy with anti-inflammatory effects) were decreased.

**Conclusions:** In ACLF, blood amino acids fueled protein and nucleotide synthesis required for the intense systemic inflammatory response. Ketogenic amino acids were extensively catabolized to produce energy substrates in peripheral organs, an effect that was insufficient because organs failed. Finally, the decrease in spermidine levels may cause a defect in autophagy contributing to the proinflammatory phenotype in ACLF.

**Lay summary:** Systemic inflammation and organ failures are hallmarks of acute-on-chronic liver failure (ACLF). Herein, we aimed to characterize the role of amino acids in these processes. The blood metabolome of patients with acutely decompensated cirrhosis, and particularly those with ACLF, reveals evidence of intense skeletal muscle catabolism. Importantly, amino acids (along with glucose), are used for intense anabolic, energy-consuming metabolism in patients with ACLF, presumably to support *de novo* nucleotide and protein synthesis in the activated innate immune system.

© 2020 European Association for the Study of the Liver. Published by Elsevier B.V. All rights reserved.

## Introduction

Several studies, including the CANONIC study,<sup>1,2</sup> the PREDICT study,<sup>3</sup> and others,<sup>4,5</sup> have shown that patients who are admitted to the hospital for an acutely decompensated cirrhosis associated with organ failure(s) and intense systemic inflammation have acute-on-chronic liver failure (ACLF). In ACLF, pathogen-associated molecular patterns (PAMPs) of bacterial origin<sup>5–7</sup> and damage-associated molecular patterns (DAMPs) released by dying cells<sup>5</sup> activate pattern-recognition receptors of the innate immune system, resulting in systemic inflammation.<sup>5,6</sup> Although systemic inflammation is certainly the primary cause of organ failures in ACLF, the mechanisms by which inflammation can perturb organ function are still unclear. These mechanisms may include tissue hypoperfusion,<sup>5</sup> alterations in cardiac function,<sup>8,9</sup>

Keywords: Multiorgan failure; Small-molecules; Biomass; Immunity; Anabolic metabolism; Dormancy.

Received 20 May 2020; received in revised form 16 November 2020; accepted 22 November 2020; available online 1 December 2020

\* Corresponding author. Address: Richard Moreau, MD, INSERM U1149, Centre de Recherche sur l'Inflammation (CRI), 16 rue Henri Huchard, 75890, PARIS cedex 18, France.

E-mail address: richard.moreau@inserm.fr (R. Moreau).

† Co-first authors

‡ Co-senior authors

<https://doi.org/10.1016/j.jhep.2020.11.035>



ELSEVIER

and immune-cell-mediated tissue damage.<sup>5</sup> Moreover, recent metabolomic results suggested that, in patients with ACLF, systemic inflammatory responses were associated with a defect in mitochondrial fatty acid-derived energy production in peripheral organs which may contribute to organ system failures.<sup>10</sup>

During sepsis under “non-cirrhotic” conditions, innate immune cells are activated and have an anabolic, energy-consuming metabolism resulting in synthesis of nucleotides, proteins and lipids that support leukocyte proliferation (increased biomass) and biosynthesis of a myriad of biomolecules involved in host defense, including, for example, soluble proteins such as cytokines, chemokines, and acute-phase proteins (Fig. S1).<sup>11–13</sup> Nutrients (e.g. glucose, amino acids) necessary to fuel immune activation<sup>11–13</sup> are mobilized from internal stores.<sup>13</sup> In addition, in activated innate immune cells, some amino acids are produced by cell-intrinsic mechanisms. Amino acids are used as building blocks for protein synthesis; 2 nonessential amino acids (glutamine and aspartate) are also substrates for *de novo* synthesis of nucleotides,<sup>14,15</sup> which are indispensable for RNA synthesis and therefore protein synthesis. Glucose extracted from blood is channeled to aerobic glycolysis to produce ATP, pyruvate, and lactate.<sup>11,13</sup> Glucose is also involved in nucleotide synthesis by giving rise to riboses (through the pentose phosphate pathway, PPP) and the nonessential amino acid serine (which is metabolized through the folate cycle).<sup>11–15</sup>

The folate cycle, and the methionine cycle are components of what is referred to as the one-carbon metabolism network.<sup>16</sup> Through the methionine cycle, the essential amino acid methionine can give rise to nucleotides among several other molecules.<sup>16,17</sup> Collectively, these findings indicate that activation of the innate immune system requires the integrated metabolism of glucose, nonessential amino acids, and one-carbon metabolism, to produce nucleotides and proteins. The different metabolic pathways are detailed in Box 1 and Figs. S2 through S5.<sup>11–19</sup>

Results of metabolomics performed in blood from patients with ACLF revealed features consistent with enhanced aerobic glycolysis and PPP in the innate immune system.<sup>10</sup> Because of the integration of glucose and amino acid metabolism in the activated innate system (Box 1; Figs. S2 through S5), we hypothesized that alterations in glucose metabolism may be associated with changes in amino acid metabolism and contribute to immune activation in ACLF. There is also evidence of enhanced catabolism of the essential amino acid tryptophan, through the kynurenine pathway, in the blood of patients with ACLF; this could give rise to metabolites that perturb peripheral-organ functions,<sup>20</sup> indicating a potential role of certain amino acids in the development of organ system failures. Of note, patients with ACLF have sarcopenia,<sup>21,22</sup> indicating intense skeletal muscle catabolism that may increase amino acid release and availability for anabolic and catabolic purposes.

### Box 1. Anabolic metabolism in activated innate immune cells.

Studies performed on sepsis under “non-cirrhotic” conditions have shown metabolic alterations, in particular alterations of the metabolisms of glucose and amino acids. At the onset of sepsis, innate immune cells, including myeloid cells (neutrophils, monocytes/macrophages, and dendritic cells) are activated because they recognize the presence of pathogen-associated molecular patterns.<sup>11–13</sup> Activated innate immune cells have an anabolic, energy-consuming metabolism resulting in synthesis of nucleotides, proteins and lipids that support leukocyte proliferation (increased biomass) and biosynthesis of a myriad of biomolecules involved in host defense, including, for example, soluble proteins such as cytokines, chemokines, and acute-phase proteins (these being produced and secreted by activated hepatocytes) (Fig. S1).<sup>11–13</sup>

Nutrients (e.g. glucose, amino acids) are necessary to fuel immune activation.<sup>11–13</sup> Because sickness behavior of anorexia is often associated with sepsis, mobilization of stored fuels is critical for survival.<sup>13</sup> Thus, during sepsis, there is activation of the hypothalamic-pituitary-adrenal axis and the sympathetic nervous system resulting in intense catabolic metabolism including, in particular, liver glycogenolysis (stimulated by adrenaline), and skeletal muscle proteolysis (stimulated by glucocorticoids), providing fuels (glucose and amino acids, respectively) to the immune system (Fig. S1).<sup>11–13</sup> In addition, in activated innate immune cells, some amino acids are produced by cell-intrinsic mechanisms.

Whatever the origin of amino acids (blood, cell-intrinsic production), these nutrients are used as building blocks for protein synthesis and in some cases as substrates for *de novo* synthesis of nucleotides (see below), which are indispensable for RNA production and therefore protein synthesis. Glucose extracted from blood is channeled to aerobic glycolysis to produce pyruvate, lactate and ATP (2 ATP per glucose molecule) (Fig. S2A). Very little pyruvate is metabolized through the mitochondrial Krebs cycle, illustrating the preference of activated cells to use glucose for anabolism (biomass buildup, production of inflammatory cues) rather than for energy production; this preference being known as the Warburg effect.<sup>12</sup> Thus, in activated innate immune cells, glucose and some non-essential amino acids play a crucial role in *de novo* nucleotide synthesis. Glucose is channeled to the pentose phosphate pathway to produce riboses and then 5-phosphoribose-1-pyrophosphate (Fig. S2A), which is a key molecule for the synthesis of purine (Fig. S2B; Fig. S3) and pyrimidine (Fig. S2C; Fig. S4) nucleotides.<sup>14,15</sup> In addition, the non-essential amino acid serine, extracted from blood or produced from an intermediate of aerobic glycolysis (Figs. S2 and S5), is channeled to the folate cycle to give rise to 1 carbon atom and the amino acid glycine, both used for nucleotide synthesis (Fig. S5).<sup>16</sup>

In activated innate immune cells, the non-essential amino acid glutamine extracted from blood is used for nucleotide synthesis both directly (Figs. S2A to S2C, S3, and S4) and indirectly. The indirect pathway leads to the production of the nonessential amino acid aspartate (Fig. S2A), which is a major contributor to *de novo* nucleotide production (Fig. S2A).<sup>14,15</sup> Thus, glutamine gives rise to  $\alpha$ -ketoglutarate which is channeled to the Krebs cycle to produce oxaloacetate used for *de novo* aspartate synthesis. Finally, it is notable that the folate cycle, mentioned earlier, and the methionine cycle are both components of what is referred to as one-carbon metabolism.<sup>16</sup> Through the methionine cycle, the essential amino acid methionine can give rise to a myriad of molecules which are crucial for immune cells.<sup>16,17</sup> These molecules include not only nucleotides but also the methyl donor S-adenosylmethionine (involved in epigenetic regulation), polyamines (that stimulate autophagy), and cystathionine (which fuels the transsulfuration pathway that gives rise to the antioxidant glutathione) (Fig. S5).

Collectively, these findings indicate that activation of the innate immune system requires the integrated metabolism of glucose, non-essential amino acids, and one-carbon metabolism, to produce nucleotides and proteins, among other effects. Proliferating cancer cells are an interesting model of biomass buildup. Indeed, proliferation of these cells relies on external nutrient supply and the integrated network of glucose, non-essential amino acid, and one-carbon metabolism, to produce nucleotides, proteins, and antioxidant molecules required for biomass production.<sup>18,19</sup>

In the current study we reanalyzed the blood metabolome data set obtained in the CANONIC study with the aim of assessing the potential role of major amino acid metabolic pathways in systemic inflammatory responses and organ failures in patients with acutely decompensated cirrhosis, with or without ACLF. Because amino acid and glucose metabolism are interrelated<sup>11,12</sup> (Fig. S2A), we used the entire metabolic data set to perform correlative and integrative analyses. We also leveraged the fact that the blood metabolome may capture important metabolic changes that occur in tissues with highly active metabolism such as activated immune cells<sup>23</sup> and cancer cells.<sup>24</sup>

## Patients and methods

### Patients

The present study used metabolomic data obtained in biobanked serum samples collected at enrollment in the CANONIC study of 831 patients with acutely decompensated cirrhosis. Part of the results of this metabolomic data set have been previously published.<sup>10,20</sup>

### Methods

#### Metabolomic data set

The data set comprised 137 well-annotated blood metabolites that had been identified using untargeted metabolomics by liquid chromatography coupled to high-resolution mass spectrometry, as previously described.<sup>10</sup> The 137 metabolites are described in Table 1 and Table S1.

#### Analysis of the data set

The strategy of analysis is described in the supplementary information, in particular the use of weighted gene co-expression network analysis (WGCNA)<sup>25,26</sup> and the computation of 9 eigenmetabolites (each being representative of a single module).<sup>10,27</sup>

For further details regarding the materials and methods used, please refer to the CTAT table and supplementary information.

## Results

### Characteristics of the study population at enrollment

There were 181 patients who had ACLF and 650 who had acute decompensation without ACLF (a group hereafter called “AD”). Table S2 summarizes baseline characteristics of patients.

### Identifying modules of related blood metabolites in acutely decompensated cirrhosis at enrollment

#### Reducing the dimension of the metabolomic data set

First, we explored the possibility that significant correlations existed between metabolites of the entire data set obtained in the whole cohort of patients with acutely decompensated cirrhosis. In fact, a large number of metabolite pairs were linked by a positive and significant correlation, with a R coefficient of 0.5 or more (Fig. S6A). Moreover, several metabolites were involved in more than 1 pair of significant correlations, suggesting the existence of groups of positively co-regulated metabolites (Fig. S6A). In contrast, very few metabolite pairs were negatively and significantly correlated, and even less were interconnected (Fig. S6B). Next, using WGCNA in the whole metabolomic data set, we identified 9 modules of co-regulated metabolites (Fig. S6C); a metabolite contained in a given module could not be present in another module. Each module

received a color name, which was arbitrarily given by the algorithm; the smallest module (magenta) contained 5 metabolites and the largest (turquoise) 28 metabolites (Table 1; Fig. 1).

#### Analysis of module membership according to categories of metabolites

We identified the presence of important categories of metabolites, including molecules related to amino acids, fatty acids, polyamines; metabolites related to glycolysis and its branch PPP; metabolites related to purines and pyrimidines, acylcarnitines; and Krebs cycle intermediates (Fig. 1; Table 1). Metabolites related to amino acids represented 43% of the metabolic data set and were the only category to be present in each of the 9 modules, although their proportion varied across modules. Amino acids and related molecules were exclusive members of the yellow module and represented the majority of metabolite members of the pink and magenta modules (86% and 80%, respectively).

#### Metabolite modules are upregulated in ACLF

Comparing eigenmetabolite values (1 per module) between patients with ACLF and those without, we found that each eigenmetabolite was significantly higher in patients with ACLF (Fig. 2). This finding is consistent with the observation that a prominent upregulation characterizes the blood metabolome of patients with ACLF.<sup>10</sup> Of note, although in each module, most members had significantly higher blood levels in ACLF relative to AD, some were not different between the 2 groups or were even significantly lower in ACLF (Table 1). These findings highlight the interest of using WGCNA for metabolomic data sets as it allowed us to include – in the same module – metabolites that may be interrelated but whose blood levels were inversely correlated.

#### In ACLF, upregulation of metabolite modules correlates with intense systemic inflammation and oxidative stress

In patients of the CANONIC cohort, we had values for white-cell count, and plasma levels of 18 protein markers of inflammation<sup>1,2</sup> (Table S1). We assessed the correlation of these variables with the 9 eigenmetabolites (Fig. 3A). Five modules or more were positively and significantly correlated with markers of systemic inflammation, including white-cell count; C-reactive protein; soluble CD163; soluble CD206; master cytokines such as interleukin (IL)-6, tumor necrosis factor  $\alpha$ , IL-10; master chemokines IL-8 (also known as C-X-C motif chemokine 8) and C-C motif chemokine 2 (also known as MCP-1). Only 4 markers of inflammation were not positively correlated with metabolite modules. Together these findings indicate that, in ACLF, metabolite module upregulation correlated with intense systemic inflammation.

The levels of human nonmercaptalbumin-2 (HNA2, which assesses irreversibly oxidized albumin<sup>2</sup>) that were also available, were increased in ACLF, consistent with systemic oxidative stress (Table S1). The 9 modules were positively correlated with HNA2 levels (Fig. 3A;  $p < 0.05$  for every correlation) indicating that, in ACLF, metabolite module upregulation correlated with systemic oxidative stress.

#### In ACLF, upregulation of metabolite modules correlates with organ system failures and severity

Correlations of the 9 eigenmetabolites with important clinical features are shown in Fig. 3B. Modules were variably correlated

**Table 1. Representative blood metabolites measured in patients with acutely decompensated cirrhosis according to their module membership, HMDB class, KEGG annotations, fold-changes in ACLF relative to AD.**

Metabolite module membership	HMDB Class	KEGG annotations (comment)	Fold-change ACLF/AD	p value
<b>Turquoise module (n = 28)</b>				
Phenylacetyl-L-glutamine	N-acyl-alpha amino acids	Phenylalanine metabolism	2.47	<0.05
N-Acetyl-ornithine	N-acyl-alpha amino acids	Arginine biosynthesis	1.23	<0.05
4-Acetamidobutanoate	Gamma amino acids and derivatives	Arginine and proline metabolism	3.60	<0.05
N6,N6,N6-Trimethyl-L-lysine	L-alpha-amino acid	Lysine degradation	1.76	<0.05
<b>N-Acetyl-L-alanine</b>	N-acyl-l-alpha-amino acids	No KEGG ID	1.85	<0.05
Hippurate	Hippuric acid (acyl glycine)	Phenylalanine metabolism.	1.66	<0.05
Quinate	Quinic acids	Phenylalanine, tyrosine and tryptophan biosynthesis.	-1.44	0.05
<b>Phenol</b>	Phenols	No KEGG pathway (HMDB: May be a product of tyrosine metabolism)	2.89	<0.05
<b>p-Anisate</b>	P-methoxybenzoic acids and derivatives.	No KEGG pathway (HMDB: Tyrosine metabolism)	4.27	<0.05
Quinoline	Pyridinecarboxylic acids	Tryptophan metabolism	3.55	<0.05
Kynurenate	Quinoline carboxylic acids	Tryptophan metabolism	2.65	<0.05
<b>Indolelactate</b>	Indolyl carboxylic acids and derivatives	No KEGG pathway (HMDB: Tryptophan catabolite)	2.39	<0.05
<b>Indoxyl sulfate</b>	Arylsulfates	No KEGG ID (HMDB: Tryptophan catabolite)	1.66	<0.05
<b>Indole-3-propionate</b>	Indolyl carboxylic acids and derivatives	No KEGG ID (HMDB: Tryptophan catabolite)	-4.53	<0.05
Methylimidazoleacetate	Imidazolyl carboxylic acids and derivatives	Histidine metabolism	2.67	<0.05
4-Hydroxy-3-methoxyphenylglycol sulfate	Methoxyphenols	No KEGG ID (HMDB: Sulfated metabolite of brain norepinephrine; marker of central norepinephrine turnover)	3.00	<0.05
Mevalonate	Hydroxy fatty acids	Terpenoid backbone biosynthesis; Ferroptosis.	2.98	<0.05
<b>N-Acetylneuraminic acid (also known as sialic acid)</b>	Carbohydrate; class of n-acylneuraminic acids	Amino sugar and nucleotide sugar metabolism.	2.24	<0.05
<b>L-(+)-Tartarate</b>	Sugar acids and derivatives	Glyoxylate and dicarboxylate.	2.37	<0.05
D-Threitol	Sugar alcohols	No KEGG pathway (Related to glucuronate pathway and pentose phosphate pathway [PPP])	3.05	<0.05
Orotidine	Pyrimidine nucleosides	No KEGG ID.	2.31	<0.05
β-Pseudouridine	Nucleoside and nucleotide analogues	Pyrimidine metabolism	2.26	<0.05
2,6-Dihydroxybenzoate	Salicylic acids	No KEGG ID (is a secondary metabolite of salicylic acid which has been hydrolyzed by liver enzymes during phase I metabolism)	1.31	<0.05
<b>Pink module (n = 7)</b>				
1-Methylhistidine (synonymous 3-Methylhistidine)	Histidine and derivatives.	Histidine metabolism	1.75	<0.05
N-Acetyl-L-phenylalanine	Phenylalanine and derivatives	Phenylalanine metabolism	2.11	<0.05
L-Kynurenine	Alkyl-phenylketones	Tryptophan metabolism	2.43	<0.05
<b>N-Acetyl-L-tryptophan</b>	n-acyl-l-alpha-amino acids	No KEGG ID (HMDB: Tryptophan metabolite converted by gut bacteria).	15.27	<0.05
<b>Indoleacetate</b>	Indole-3-acetic and derivatives	Tryptophan metabolism (HMDB: May be converted by gut bacteria)	1.85	<0.05
<b>Magenta module (n = 5)</b>				
Cystathionine	L-cysteine-s-conjugates	Cysteine and methionine metabolism	2.98	<0.05
L-Saccharopine	Glutamic acid and derivatives.	Lysine degradation	5.80	<0.05
N-Acetylaspartilglutamate (NAAG)	Dipeptides	Alanine, aspartate and glutamate metabolism	3.00	<0.05
Arginine succinate	Aspartic acid and derivatives	Arginine biosynthesis; Alanine, aspartate and glutamate metabolism	1.54	<0.05
<b>Green module (n = 14)</b>				
N-Acetyl-L-tyrosine	Tyrosine and derivatives	No KEGG pathway T(HMDB: Tyrosine metabolism)	2.32	<0.05
<b>N-Formyl-L-methionine</b>	Methionine and derivatives	Cysteine and methionine metabolism	1.68	<0.05
5'-Deoxy-5'-(methylthio)adenosine (S-Methyl-5'-thioadenosine)	5'-deoxy-5'-thionucleosides	Cysteine and methionine metabolism	3.01	<0.05
<b>Phenyllactate</b>	Phenylpropanoic acids	Phenylalanine metabolism.	2.41	<0.05

(continued on next page)

Table 1. (continued)

Metabolite module membership	HMDB Class	KEGG annotations (comment)	Fold-change ACLF/AD	p value
<b>p-Hydroxyphenyllactate</b>	Phenylpropanoic acids	No KEGG pathway (HMDB: Tyrosine metabolite).	1.96	<0.05
D-Xylulose 5-phosphate/D-Ribulose 5-phosphate/D-Ribose 1-phosphate/D-Ribose 5-phosphate <sup>a</sup>	Pentose phosphates	PPP	5.46	<0.05
<b>D-Galacturonate</b>	Glucuronic acid derivatives	Pentose and glucuronate interconversions	3.95	<0.05
D-Glucuronate	Glucuronic acid derivatives	Pentose and glucuronate interconversions	2.40	<0.05
2-Hydroxyhexadecanoate	Long-chain fatty acids	No KEGG pathway	1.52	<0.05
Adenine	6-aminopurines	Purine metabolism	1.57	<0.05
<b>Black module (n = 9)</b>				
Hexanoylcarnitine	Acylcarnitines	No KEGG pathway	2.30	<0.05
Octanoylcarnitine	Acylcarnitines	No KEGG pathway	1.89	<0.05
Decanoylcarnitine	Acylcarnitines	No KEGG pathway	1.53	<0.05
Butyrylcarnitine	Acylcarnitines	No KEGG pathway	1.77	<0.05
<b>2-Heptanone</b>	Ketones	No KEGG pathway	6.65	<0.05
N8-Acetylspermidine	Carboximidic acids	No KEGG pathway (HMDB: Polyamine metabolism)	1.51	<0.05
<b>Brown module (n = 21)</b>				
Pyruvate	Alpha-keto acids and derivatives	Glycolysis	1.28	<0.05
Citrate/Isocitrate <sup>a</sup>	Tricarboxylic acids and derivatives	Citrate cycle (also known as tricarboxylic acid cycle, Krebs' cycle)	1.29	<0.05
Aconitate	Tricarboxylic acids and derivatives	Citrate cycle (also known as tricarboxylic acid cycle, Krebs' cycle)	1.50	<0.05
α-Ketoglutarate (also known as 2-Oxo glutarate)	Gamma-keto acids and derivatives	Citrate cycle (also known as tricarboxylic acid cycle, Krebs' cycle)	1.26	<0.05
Succinate/Methylmalonate <sup>a</sup>	Dicarboxylic acids and derivatives	Citrate cycle (also known as tricarboxylic acid cycle, Krebs' cycle)	1.67	<0.05
Malate/Diglycolate <sup>a</sup>	Malic acid belongs to the class of beta hydroxy acids and derivatives	Malic acid is a Krebs' cycle intermediate (Here, the presence of diglycolic acid is highly unlikely because it is a product of diethylene glycol)	1.38	<0.05
Oxaloacetate	Short-chain keto acids and derivatives.	Citrate cycle (also known as tricarboxylic acid cycle, Krebs' cycle); Glycolysis	1.42	<0.05
N-Acetyl-L-aspartate	Aspartic acid and derivatives	Alanine, aspartate and glutamate metabolism	1.51	<0.05
Carnitine	Carnitines	Lysine degradation	1.19	<0.05
Creatine	Alpha amino acids and derivatives.	Arginine and proline metabolism	1.71	<0.05
2-Aminoisobutyrate	Alpha amino acids	No KEGG pathway	1.30	<0.05
2-Oxovalerate	Short-chain keto acids and derivatives	No KEGG pathway	1.40	<0.05
<b>Blue module (n = 23)</b>				
Lactate	Alpha hydroxy acids and derivatives	Glycolysis.	1.39	<0.05
D-Glycerate	Sugar acids and derivatives	PPP; Glycerolipid metabolism; Glycine, serine and threonine metabolism	1.43	<0.05
L-Citrulline	L-alpha-amino acids	Arginine biosynthesis	1.23	<0.05
Glutamine	L-alpha-amino acids. Proteinogenic amino acid.	Arginine biosynthesis; Purine metabolism; Pyrimidine metabolism; Alanine, aspartate and glutamate metabolism	1.15	<0.05
Glutamate	Glutamic acid and derivatives. Proteinogenic amino acid.	Arginine biosynthesis; Arginine and proline metabolism; Alanine, aspartate and glutamate metabolism; Taurine and hypotaurine metabolism; Glutathione metabolism; Ferroptosis	1.13	0.05
Aspartate	Aspartic acid and derivatives. Proteinogenic amino acid.	Arginine biosynthesis; Cysteine and methionine metabolism; Alanine, aspartate and glutamate metabolism	-1.03	0.77
L-Cystine	L-cysteine-s-conjugates	Cysteine and methionine metabolism; Ferroptosis.	1.29	<0.05
5-Hydroxylysine	L-alpha-amino acids.	Lysine degradation	1.22	<0.05
N6-Acetyl-L-lysine	L-alpha-amino acids.	Lysine degradation	1.35	<0.05

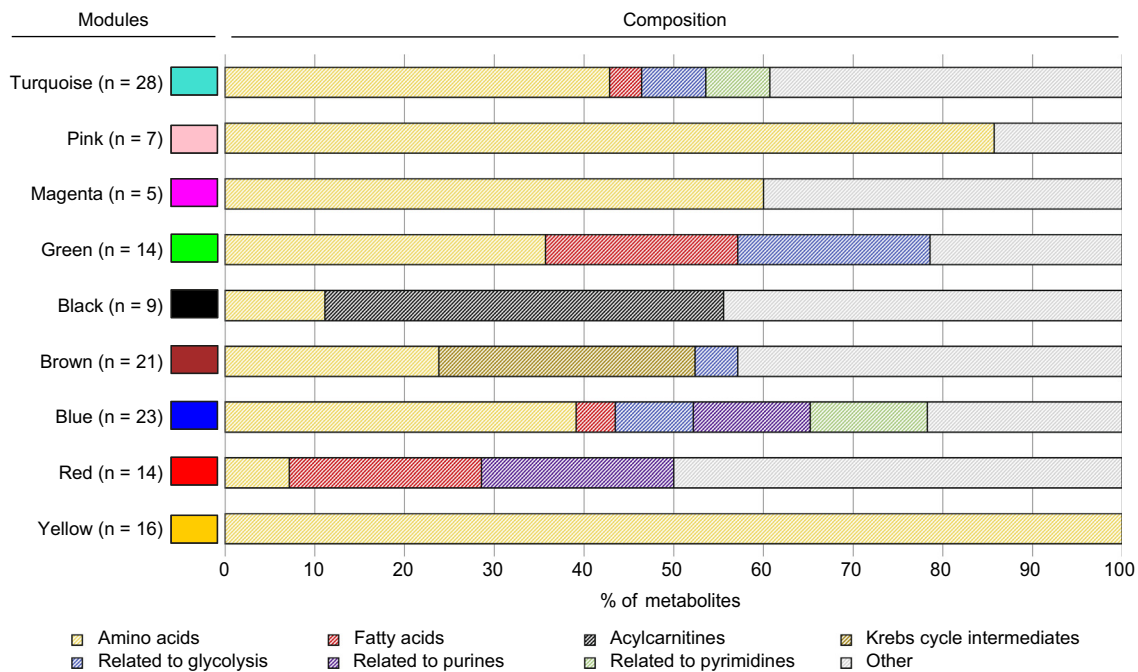
(continued on next page)

Table 1. (continued)

Metabolite module membership	HMDB Class	KEGG annotations (comment)	Fold-change ACLF/AD	p value
Pyroglutamate (5-Oxoproline)	Alpha amino acids and derivatives	Glutathione metabolism	1.14	<0.05
Spermidine	Dialkylamines	Polyamine; Arginine and proline metabolism; Glutathione metabolism; beta-alanine metabolism	-1.30	<0.05
Thymine	Hydroxypyrimidines (pyrimidine derivatives)	Pyrimidine metabolism	1.09	<0.05
Dihydrothymine	Hydroxypyrimidines (pyrimidine derivatives)	Pyrimidine metabolism	1.35	<0.05
Orotate	Pyrimidinecarboxylic acids (pyrimidine derivatives)	Pyrimidine metabolism	1.65	<0.05
Hypoxanthine	Hypoxanthines (purine derivatives)	Purine metabolism	1.08	0.42
Xanthine	Xanthines (purine derivatives)	Purine metabolism	-1.10	0.11
Inosine	Purine nucleosides	Purine metabolism	-1.11	0.45
Taurine	Organosulfonic acids	Taurine and hypotaurine metabolism; Sulfur metabolism	1.05	0.22
Choline	Cholines	Glycerophospholipid metabolism	1.02	0.56
<b>Red module (n = 14)</b>				
Allantoin	Imidazole	Purine metabolism	1.37	<0.05
Urate	Xanthines	Purine metabolism	1.14	<0.05
Oxalate	Dicarboxylic acids and derivatives	Purine metabolism; Glyoxylate and dicarboxylate metabolism	1.05	0.39
Glycerol 3-phosphate	Glycerophosphates	Glycerolipid metabolism; Glycerophospholipid metabolism	1.17	<0.05
Phenylpyruvate	Phenylpyruvic acid derivatives	Phenylalanine metabolism	-1.42	<0.05
Isobutyrate	Carboxylic acids	Microbial metabolism in diverse environments	1.21	<0.05
Threonate	Sugar acids and derivatives	Ascorbate and aldarate metabolism	1.31	<0.05
<b>Yellow module (n = 16)</b>				
Serine	Serine and derivatives. Proteinogenic amino acid.	Glycine, serine and threonine metabolism; Cysteine and methionine metabolism; Sphingolipid metabolism	-1.07	<0.05
Methionine	Methionine and derivatives. Proteinogenic amino acid.	Cysteine and methionine metabolism	1.38	<0.05
Methionine sulfoxide (L-Methionine S-oxide)	L-alpha-amino acids.	Cysteine and methionine metabolism	1.82	<0.05
Arginine	L-alpha-amino acids. Proteinogenic amino acid.	Arginine biosynthesis; Arginine and proline metabolism	1.12	<0.05
Ornithine	L-alpha-amino acids	Arginine biosynthesis; Arginine and proline metabolism	1.25	<0.05
Proline	Proline and derivatives. Proteinogenic amino acid.	Arginine and proline metabolism	1.15	<0.05
Phenylalanine	Phenylalanine and derivatives. Proteinogenic amino acid.	Phenylalanine metabolism; Phenylalanine, tyrosine and tryptophan biosynthesis	1.36	<0.05
Tyrosine	Tyrosine and derivatives. Proteinogenic amino acid.	Tyrosine metabolism; Phenylalanine metabolism; Phenylalanine, tyrosine and tryptophan biosynthesis	1.16	<0.05
Threonine/D-allo-Threonine <sup>a</sup>	No overlapping class	Not applicable	1.00	1.00
Isoleucine	Isoleucine and derivatives. Proteinogenic amino acid.	Valine, leucine and isoleucine degradation; Valine, leucine and isoleucine biosynthesis. Branched amino acid (with valine and leucine)	1.14	<0.05
β-Alanine/Alanine/Sarcosine <sup>a</sup>	No overlapping class.	Not applicable	1.17	<0.05
Asparagine	Asparagine and derivatives. Proteinogenic amino acid.	Alanine, aspartate and glutamate metabolism	1.10	<0.05
Lysine	L-alpha-amino acids. Proteinogenic amino acid.	Lysine degradation, lysine biosynthesis	1.18	<0.05
Histidine	Histidine and derivatives. Proteinogenic amino acid.	Histidine metabolism, β-alanine metabolism	1.10	<0.05
Tryptophan	Indolyl carboxylic acids and derivatives. Proteinogenic amino acid.	Tryptophan metabolism, Phenylalanine, tyrosine and tryptophan biosynthesis	1.09	0.11
Allantoate	N-carbamoyl-alpha amino acids	Purine metabolism	1.05	0.22

<sup>a</sup>This study is a reanalysis of the CANONIC metabolomic data set previously published.<sup>1</sup> The comprehensive list of the 137 metabolites included in the data set is provided in Table S1. Metabolite annotation was obtained using HMDB, KEGG databases and references #10 through #20, #23, #24, #32, #34 through #37. Metabolites in bold are those of potential bacterial origin.<sup>10</sup> p values were obtained using the Student's *t* test for unpaired data. ACLF, acute-on-chronic liver failure; AD, acute decompensation without ACLF; HMDB, Human Metabolome Database ([www.hmdb.ca](http://www.hmdb.ca)); KEGG, Kyoto Encyclopedia of Genes and Genomes. [www.genome.jp/kegg](http://www.genome.jp/kegg).

<sup>a</sup>Some isomeric metabolites could not be resolved using the liquid chromatography coupled to high-resolution mass spectrometry approach.<sup>1</sup>



**Fig. 1. Metabolite module membership.** Distribution of metabolite members of each module according to metabolite categories detailed in Table 1. Metabolites related to amino acids are the only category to be present across the 9 modules. (This figure appears in color on the web.)

with age. A large number of modules were positively, and significantly, correlated with serum bilirubin, international normalized ratio (INR), and plasma renin concentration. Consistent with findings related to plasma renin, several modules were negatively and significantly correlated with mean arterial pressure. The results therefore indicated that upregulation of a large number of modules seen in ACLF, was closely associated with worsening in liver, coagulation (which primarily reflects liver failure), kidney, and circulatory functions. Of note, 3 modules were correlated positively and significantly with increasing hepatic encephalopathy (HE) grades, indicating that changes in the blood metabolome were less related to brain failure than the other major organ system failures. Finally, we found that the 9 modules were positively and significantly correlated with the “global” CLIF-C organ failure score, the increasing number of failing organ systems, and the increasing ACLF grade, confirming that module upregulations paralleled the increase in disease severity.

*Addressing the role of deteriorating kidney function on blood metabolite accumulation*

Kidney dysfunction or failure are highly prevalent in patients with acutely decompensated cirrhosis (Table S1). A deterioration in kidney function might result in decreased renal metabolite excretion and accordingly contribute to blood metabolite accumulation. Indeed, eigenmetabolites were significantly correlated with serum creatinine (Fig. 3B) and increased in the presence of kidney dysfunction (Fig. S7). However, among patients with ACLF, only 2 eigenmetabolites (turquoise and pink modules) were upregulated in patients with single kidney failure, relative to those without kidney failure (Fig. S7). Moreover, the 9 eigenmetabolites were positively and significantly correlated with bilirubin and INR, suggesting a relationship with liver failure (Fig. 3B). Together,

these findings suggested that the levels of blood metabolites may not depend only on the deterioration of kidney function. Therefore, we computed a multivariate analysis evaluating the independent correlations of each metabolite of each module with serum creatinine, serum bilirubin, and the grades of HE. We found that 50% to 100% of metabolites of each of the 9 modules (therefore including the yellow module) were independently and positively correlated with creatinine (Fig. S8A). We also found that 40% to 100% of metabolites of each of the 9 modules were independently and positively correlated with bilirubin (Fig. S8A). In addition, a variable proportion of the metabolites of 5 modules were independently and positively correlated with increasing HE grades (Fig. S8A). A large majority of metabolites (69%) were independently correlated with deterioration of 2 organs (50% of metabolites) or 3 organs (19% of metabolites) (Fig. S8B; Table S3). Nine percent of the 137 metabolites were not correlated with either of the 3 organs. Collectively, these findings suggested that blood metabolite accumulation in ACLF was not a simple consequence of a reduction in renal excretion of metabolites but the result of several independent effects. The multivariate analysis also revealed that among the 137 metabolites, 78% were independently correlated with creatinine, 73% with bilirubin and 28% with HE grade, confirming that changes in blood metabolome were more closely associated with deterioration of kidney or liver functions than with deterioration of brain function.

*Addressing the association with precipitating events*

Among patients with ACLF, we compared the 9 eigenmetabolites measured at enrollment, between patients who had bacterial infection as a precipitating event and those without. Four eigenmetabolites (turquoise, magenta, green, and black) were significantly higher in patients with bacterial infection while the remaining eigenmetabolites did not differ between the 2 groups

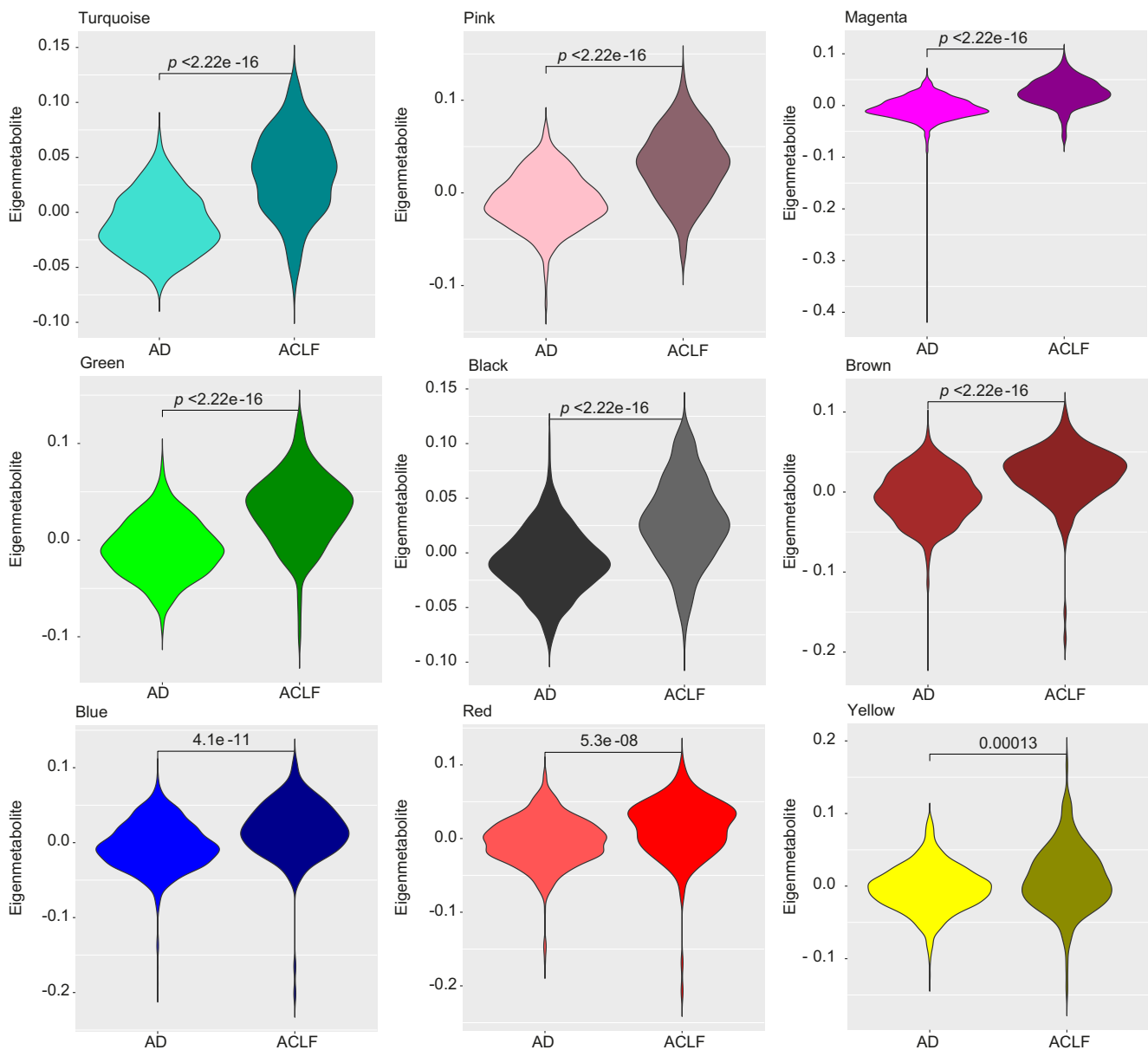


**Fig. 2. Metabolite modules are upregulated in ACLF** Comparison of the eigenmetabolite value of each of the 9 metabolite modules, between patients with ACLF and those with AD. *p* values were obtained using the Student's *t* test for unpaired values. ACLF, acute-on-chronic liver failure; AD, acute decompensation without ACLF. (This figure appears in color on the web.)

(Fig. S9A). We identified 13 metabolites of potential bacterial origin in 3 modules associated with infection (8 metabolites in the turquoise module, 4 in the green module, and 1 in the black module) (Table 1). Among patients with ACLF, we also performed the comparison for 2 other precipitating events, excessive alcohol consumption and gastrointestinal hemorrhage, and found no differences in eigenmetabolites with each of these events (Fig. S9B and S9C).

*Antecedence of metabolite module upregulation relative to ACLF development and death*

Among the patients with AD (without ACLF) at enrollment, we wondered whether the blood metabolome at that time differed between those who would go on to develop ACLF by

28 days (*n* = 69) and those who would not (*n* = 536). We compared the 2 groups using the 9 eigenmetabolites measured at enrollment and found that, except for the red-module eigenmetabolite, every eigenmetabolite was significantly higher among patients who developed ACLF by 28 days than among those who did not (Fig. S10). We found that the same 8 eigenmetabolites were significantly higher at enrollment, among patients who died within 28 days (*n* = 79) than among those who survived (*n* = 752) (Fig. S11). The remaining eigenmetabolite (red module) did not differ between the 2 groups. Collectively, these findings indicated that metabolite module upregulation at enrollment preceded the short-term occurrence of major outcomes such as the development of ACLF and death.



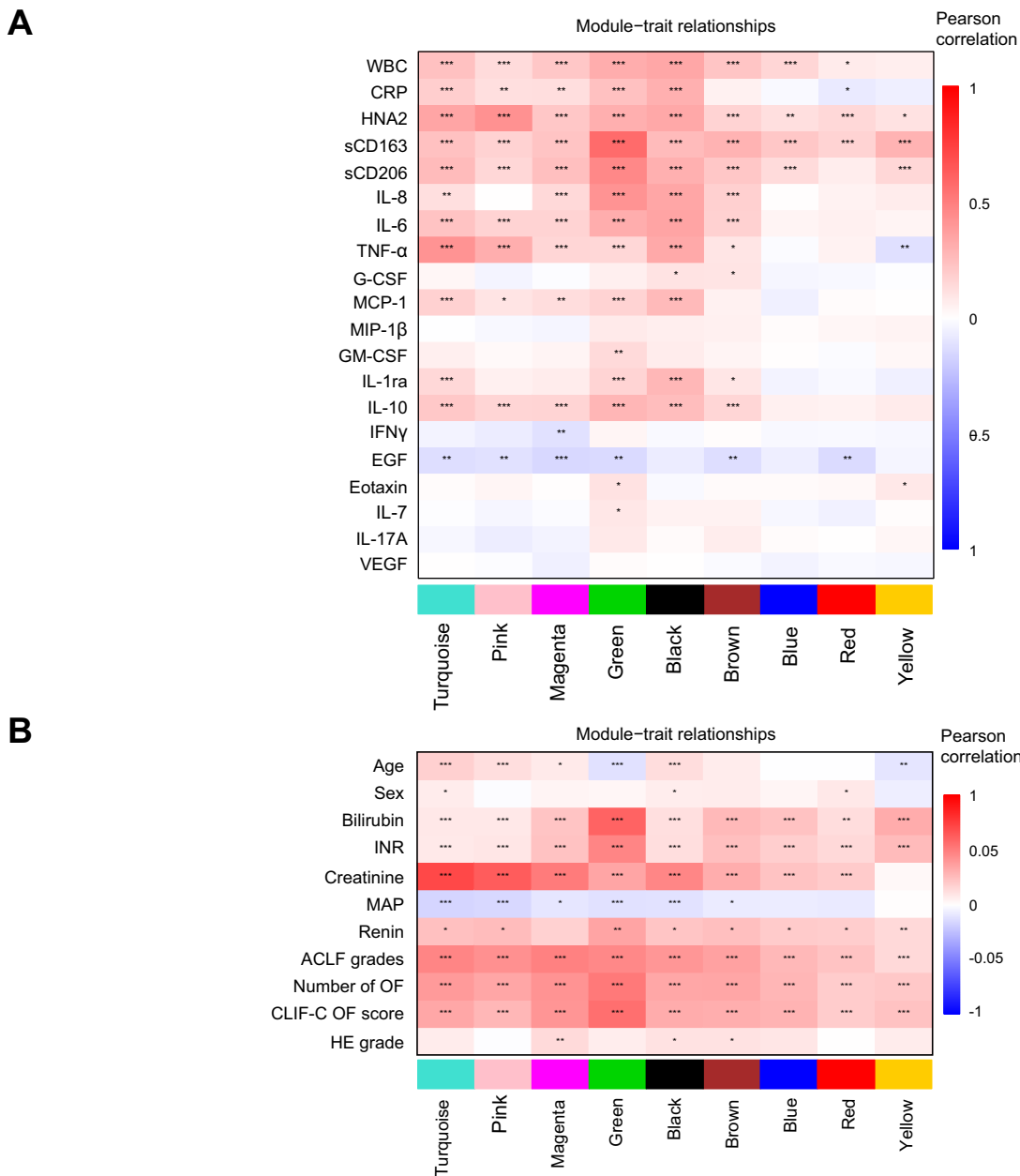


**Fig. 3. In ACLF, upregulation of metabolite modules correlates with intense systemic inflammation and oxidative stress and organ system failures.** (A) Heatmap of the pairwise Pearson correlation coefficients between the metabolite modules and markers of systemic inflammation (including white-cell count, and plasma levels of 18 proteins) and oxidative stress (HNA2). Full list of abbreviations are defined in Table S1. (B) Heatmap of the pairwise Pearson correlation coefficients of the metabolite modules and important clinical markers. In (A) and (B), empty cells indicate correlations which were not significant. \* $p < 0.05$ ; \*\* $p < 0.01$ ; \*\*\* $p < 0.001$ . ACLF, acute-on-chronic liver failure; HNA2, human nonmercaptalbumin-2. (This figure appears in color on the web.)

**Antecedence of changes in individual metabolites relative to death**  
 We asked whether the blood levels of paradigmatic metabolites assessed at enrollment would be associated with patient outcomes. The levels of methionine, those related to aerobic glycolysis (pyruvate and lactate), and those related to PPP (pentose phosphates, glucuronate, galacturonate) were significantly higher among patients who died within 28 days than among those who survived (Fig. S12). In contrast, the levels of the polyamine spermidine were significantly lower among patients who died within 28 days (Fig. S12). These findings suggest an important prognostic role for the metabolism of

methionine, glycolysis, PPP, and spermidine, in patients with acutely decompensated cirrhosis. In addition, our results indicate that the prognostic value of individual paradigmatic metabolites was generally related to the increases in their blood levels, and for spermidine to the decreases in their blood levels.

**Potential multiple roles of amino acids in ACLF**

*Proteinogenic amino acids are mobilized in ACLF*

We first analyzed the yellow module, which exclusively comprised amino acids ( $n = 16$ ). Of these, the blood levels of 12

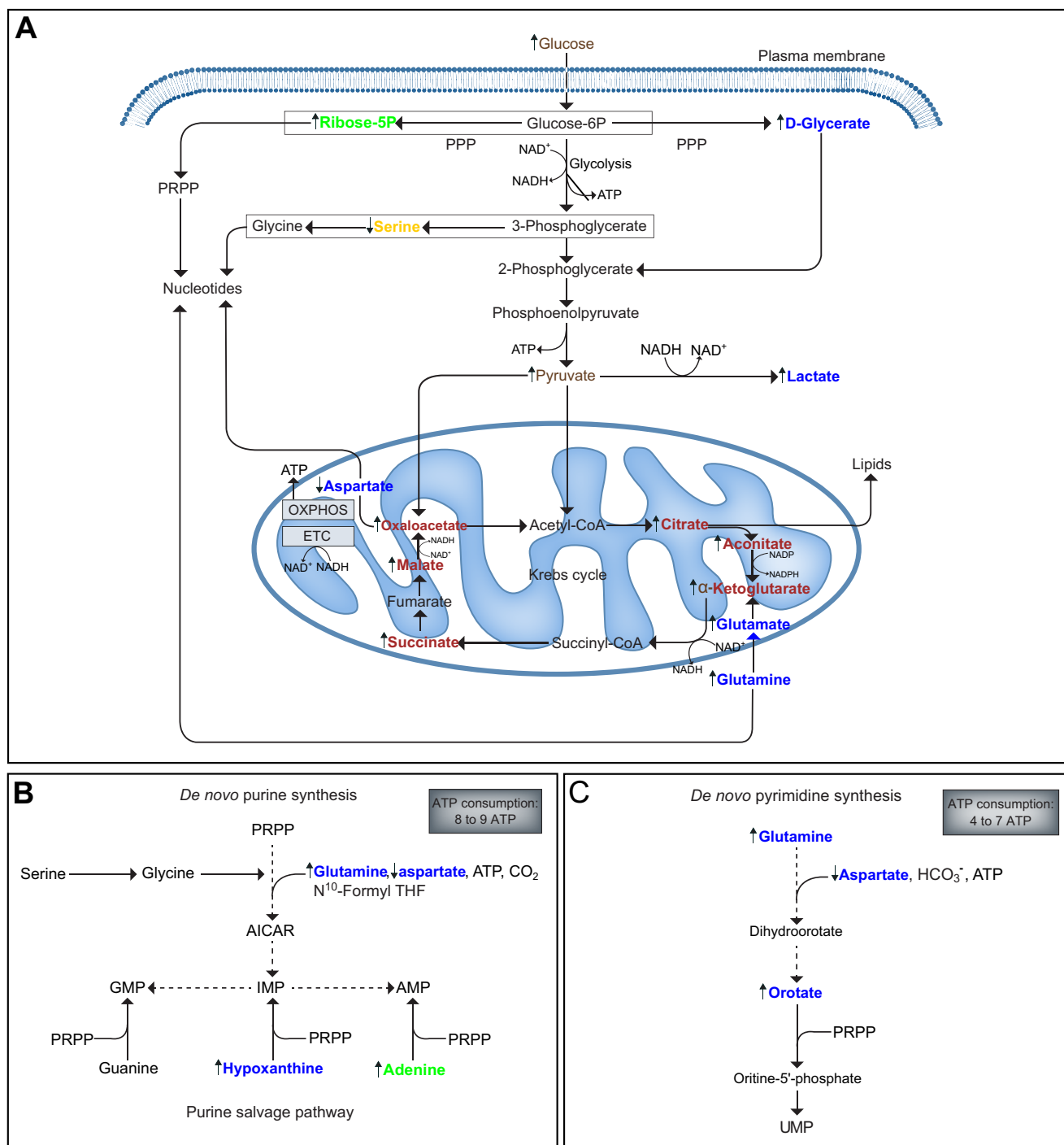


**Fig. 4. Modeling of nucleotide synthesis in ACLF.** (A) Schematic of central carbon metabolism through glycolysis and Krebs cycle. (B) Schematic of *de novo* and salvage purine synthesis. (C) Schematic of *de novo* and salvage pyrimidine synthesis. (B,C) Estimated ATP consumption necessary for synthesis of the corresponding nucleotides. (A-C) Enzymes involved in the pathways illustrated here are not shown. (A-C) Members of metabolite modules developed from the CANONIC database are shown using the color of the corresponding module. Direction of arrows indicates metabolite up- or downregulation. For details, please see Figs. S2 through S4. ACLF, acute-on-chronic liver failure; ETC, electron transport chain; OXPHOS, oxidative phosphorylation; PPP, pentose phosphate pathway; PRPP, 5-phosphoribose-1-pyrophosphate. (This figure appears in color on the web.)

members were higher in ACLF than AD (Table 1). Together, these findings suggested an orchestrated regulation of blood levels of yellow-module members. Among the yellow-module members, 11 (including serine, methionine, arginine, proline, phenylalanine, tyrosine, isoleucine, lysine, asparagine, histidine, and

tryptophan) were proteinogenic amino acids, *i.e.* molecules that are incorporated into proteins under mRNA direction. In the context of inflammation, proteinogenic amino acids can also be used for catabolic purposes, as shown in other parts of the Results section and previous studies<sup>13</sup> (Fig. S1).

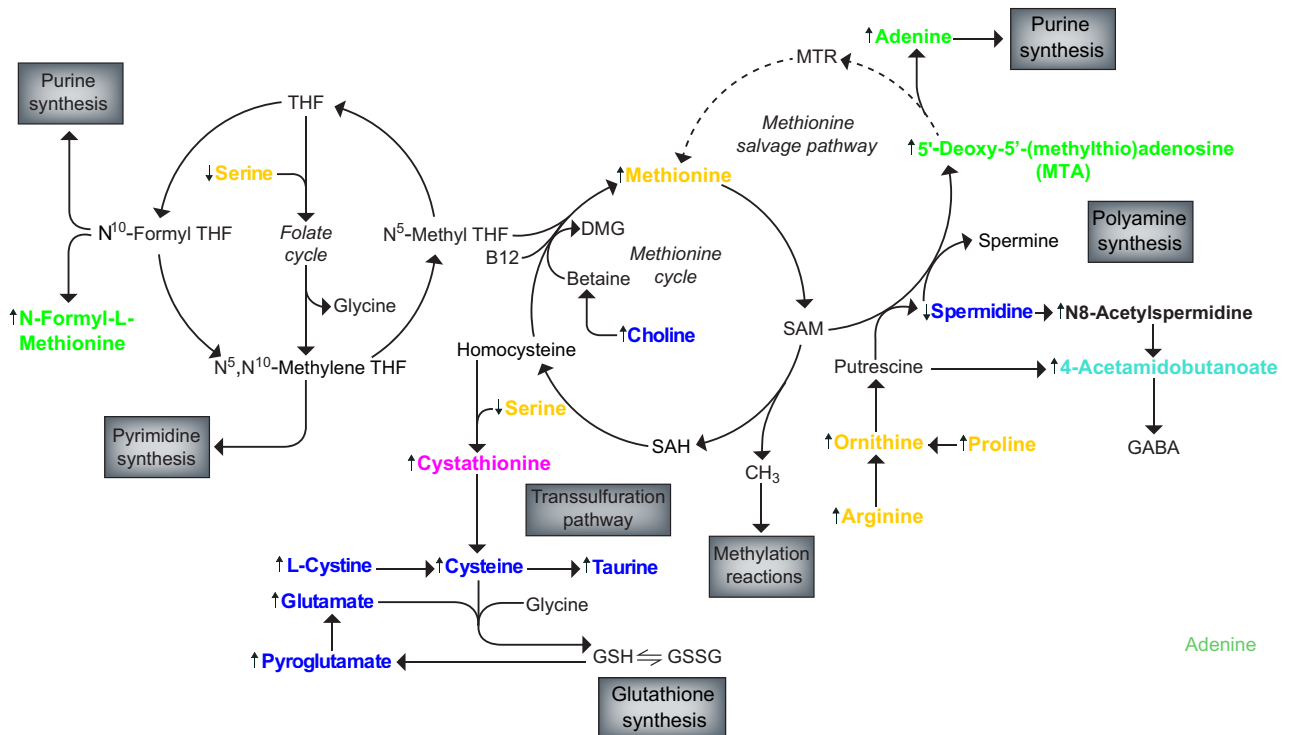


**Fig. 5. Modeling the one-carbon metabolic network in ACLF.** The one-carbon metabolic network comprises the folate cycle and the methionine cycle. Enzymes involved in the one-carbon metabolic network are not shown. Members of metabolite modules developed from the CANONIC data base are shown using the color of the corresponding module. Direction of arrows indicates metabolite up- or down-regulation. For details, please see Figs. S2 through S4. ACLF, acute-on-chronic liver failure; DMG, dimethylglycine; GSH, reduced glutathione; GSSG, oxidized glutathione; MTA, 5'-deoxy-5'-(methylthio)adenosine; MTR, methylthioribose; SAM, S-adenosylmethionine; SAH, S-adenosylhomocysteine; THF, tetrahydrofolate. (This figure appears in color on the web.)

**Modeling the role of amino acids in nucleotide synthesis in ACLF**  
 ACLF associates with enhanced aerobic glycolysis, PPP, and nucleotide synthesis. In ACLF, as expected,<sup>10</sup> there was blood accumulation of pyruvate and lactate. Although pyruvate and lactate had different module membership (brown module and blue module, respectively [Table 1]), a finding that may be explained by the fact that pyruvate can give rise not only to lactate but also acetyl-CoA, and oxaloacetate, among others<sup>19</sup> (Fig. S2A), lactate and pyruvate levels were positively and significantly correlated (Fig. S13A), indicating increased aerobic glycolysis (Fig. 4A). In addition, ACLF was associated with increased blood levels of metabolites related to the branch of glycolysis and PPP, including ribose-5-phosphate (green module; Fig. 4A), indicating that glucose-6-phosphate was also channeled to PPP (Fig. 4A). Of note, the levels of pyruvate (Fig. S13B) and lactate (Fig. S13C) were significantly and positively correlated with the levels of pentose phosphates and metabolites related to PPP (glucuronate, galacturonate, both green-module members), consistent with the simultaneous activation of aerobic glycolysis and PPP in ACLF. In addition, we found that N-formyl-L-methionine (green module), a reporter of N<sup>10</sup>-formyl tetrahydrofolate synthesis,<sup>14</sup> was increased in ACLF, suggesting an increased conversion of serine to glycine and formate (one-carbon) production in the folate cycle (Fig. 5). In addition, the blue module was enriched with several molecules involved in nucleotide synthesis, including glutamine, aspartate, xanthine and hypoxanthine (purine bases involved in purine salvage; Fig. 4B);

inosine (the hypoxanthine nucleoside); orotate (whose production is coupled to ETC and gives rises to pyrimidine ring; Fig. 4C); thymine (a pyrimidine base) and its derivative (dihydrothymine). Several Krebs cycle intermediates (all in the brown module), e.g.  $\alpha$ -ketoglutarate and oxaloacetate (which gives rise to aspartate [Fig. 4A]), were increased in ACLF. Of note, investigating positively correlated eigenmetabolites, we identified an ordered network of metabolite modules showing, in particular, a structure with the following order yellow-blue-brown-green (Fig. S14), suggesting a close co-orchestration of these 4 modules. Of note, we found evidence in ACLF of increased methionine cycle and its branch the methionine salvage pathway (see below) which may contribute to the increased levels of adenine (green module; Table 1; Fig. 5), a substrate for salvage purine synthesis (Fig. 4B), in ACLF. Collectively, our findings suggested that, in ACLF, there was an orchestrated activation of aerobic glycolysis and PPP, one-carbon metabolic network (involving the folate cycle and methionine cycle), and Krebs cycle with the objective of fueling purine synthesis (*de novo* and salvage), and *de novo* pyrimidine synthesis. These findings were reminiscent of those in activated innate immune cells wherein aerobic glycolysis and nucleotide synthesis are stimulated<sup>14</sup> (Fig. S2A). Because innate immunity is activated in ACLF, the blood metabolome in patients with ACLF may capture metabolites related to enhanced nucleotide synthesis, which is required to produce biomass (leukocytosis) and a broad variety of inflammatory mediators in the innate immune system.

### Modeling methionine metabolism in ACLF

Next, we investigated the methionine cycle, the second component of the one-carbon metabolic network<sup>16</sup> (Fig. 5).

ACLF associates with activation of the transsulfuration and methionine salvage pathways. Our patients with ACLF had several features consistent with the engagement of the methionine cycle. First, they had blood accumulation of methionine (yellow module). Second, they had evidence of an activated transsulfuration pathway, indicated by blood accumulation of cystathionine (magenta module) and L-cystine, pyroglutamate, and glutamate (all involved in glutathione synthesis [Fig. 5] and blue-module members). Taurine, the other product of the transsulfuration pathway, was a blue-module member, but its levels did not significantly differ between ACLF and AD (Table 1), suggesting that glutathione production was prioritized in ACLF. Together, our results suggest that part of homocysteine was skewed towards cystathionine and the transsulfuration pathway. Third, patients with ACLF had increased blood levels of 5'-deoxy-5'-(methylthio)adenosine (MTA) indicating engagement of the methionine salvage pathway. Collectively, our results suggest that, in ACLF, priority was given to both the production of the antioxidant glutathione via the transsulfuration pathway and methionine renewal via the methionine salvage pathway. Our finding that choline was contained in the blue module might suggest that choline was channeled to produce methionine and therefore contribute to methionine re-synthesis (Fig. 5). The engagement of metabolic pathways whose purpose is methionine renewal suggests a pivotal role of methionine in ACLF. In addition, the fact that adenine levels were increased in ACLF and that both MTA and adenine were green-module members, suggest that the methionine salvage pathway was used to fuel the purine salvage pathway (Fig. 5). Of note, our finding of a network comprising the yellow-blue-brown-green modules (Fig. S14), was also consistent with methionine fueling the flux backbone of one-carbon metabolism.

We also observed decreased levels of the polyamine spermidine and accumulation of GABA precursors in blood from patients with ACLF. In ACLF, the levels of the putrescine-precursor ornithine, and those of the polyamine synthesis byproduct MTA, were increased, suggesting increased polyamine synthesis (Fig. 5). However, in ACLF, spermidine levels were not increased but significantly decreased (Table 1) and spermine was undetectable. The decrease in spermidine may be explained, at least in part by the conversion of spermidine into N8-acetylspermidine (black module; Table 1; Fig. 5). Of note, N8-acetylspermidine and putrescine can give rise to 4-acetamidobutanoate (turquoise module; Fig. 5) whose levels were increased in ACLF relative to AD (Table 1). 4-acetamidobutanoate is an immediate precursor of 4-aminobutanoate (also known as GABA), a master mediator of GABAergic neurons. Neuroinflammation-induced activation of the GABAergic system has been shown to contribute to features of hepatic encephalopathy.<sup>28</sup> Collectively, these findings might suggest that N8-acetylspermidine via 4-acetamidobutanoate might fuel the GABAergic nervous system in acutely decompensated cirrhosis. However, this hypothesis would require confirmation because in the metabolite module network (Fig. S14), the modules containing each of these metabolites (black and turquoise, respectively) were not significantly correlated. Moreover, of the 2 metabolites, only N8-acetylspermidine

but not 4-acetamidobutanoate, was independently and significantly correlated with HE grade (Table S3).

*ACLF associates with blood accumulation of ketogenic amino acids*  
In ACLF, glucose is prioritized to immune cells at the expense of peripheral organs.<sup>10</sup> In the context of PAMP- or DAMP-induced systemic inflammation, ketone bodies (acetoacetate,  $\beta$ -hydroxybutyrate) become an important source of energy in peripheral organs.<sup>11</sup> Oxidation of fatty acids and amino acids, which are mobilized from adipose tissue and skeletal muscle, respectively, usually support ketogenesis.<sup>13</sup> Our patients with ACLF had lipolysis as indicated by blood accumulation of free fatty acids, for example 2-hydroxyhexadecanoate, a product of lipolysis (green module). However, these patients also had blood accumulation of acylcarnitines (*i.e.* fatty acids attached to carnitine) (Table 1), indicating the inhibition, in peripheral organs, of the translocation of these molecules into mitochondria.<sup>10,13,23</sup> Therefore, in peripheral organs, there was a suppression of fatty acid  $\beta$ -oxidation and ATP synthesis, which may contribute to organ failures. In addition to fatty acids, amino acids, including isoleucine, lysine, tryptophan, leucine, tyrosine, and phenylalanine (Fig. S15A), can serve as substrates for synthesis of ketone bodies.<sup>13</sup> In our study, all ketogenic amino acids but leucine were in the yellow module; of these, the levels of isoleucine, lysine, tyrosine, and phenylalanine were increased in the blood in ACLF, while levels of tryptophan did not differ in ACLF vs. AD (Table 1). Moreover, in ACLF, we observed blood accumulation of catabolites of phenylalanine and tyrosine (Fig. S15B), tryptophan (Fig. S16), and lysine (Table 1). However, in ACLF, although there was extensive ketogenic amino acid catabolism, the canonical ketone body,  $\beta$ -hydroxybutyrate,<sup>13</sup> was not identified in our metabolomic data set, raising the hypothesis that ACLF was associated with a defect in or an inhibition of ketone body production from amino acids.

### Discussion

This study reanalyzed the metabolomic data set (comprising 137 metabolites) obtained from samples of the CANONIC study,<sup>10</sup> a study which enrolled a large cohort of patients with acutely decompensated cirrhosis.<sup>1</sup> Using the entire metabolomic data set obtained in the whole cohort, we identified 9 metabolite modules, each containing highly correlated molecules and each receiving an arbitrary color label. Unlike other metabolites, amino acids were present in every module, highlighting the important contribution of these molecules to the blood metabolome. Each module, assessed via its eigenmetabolite, was upregulated in ACLF relative to AD, confirming that blood metabolome changes in ACLF are characterized by prominent metabolite accumulation, although some individual metabolites decreased (*e.g.* spermidine).<sup>10</sup> Several eigenmetabolites were positively and significantly correlated with *bona fide* markers of systemic inflammation, indicating that metabolic changes paralleled the intensity of systemic inflammation. The 9 eigenmetabolites were positively correlated with markers of overall severity. Among patients with ACLF, some eigenmetabolites were higher in infected than in noninfected modules and the corresponding modules contained metabolites of potential bacterial origin. Finally, we found that 8 eigenmetabolites measured at enrollment in patients with AD, were significantly higher among those who developed ACLF during follow-up than among those who remained free of ACLF. These 8 eigenmetabolites were

significantly higher in patients who died within 28 days than among patients who remained alive. Moreover, we found that some individual paradigmatic metabolites significantly differed between patients who died and those who remained alive. These findings indicated the antecedence of eigenmetabolite upregulation, or changes in the expression of individual metabolites, relative to poor clinical outcome and suggest that blood metabolites should be evaluated as prognostic biomarkers in future studies.

In univariate analysis, 8 eigenmetabolites were positively correlated with kidney failure, suggesting that blood metabolite accumulation in ACLF may be a passive result of defective renal excretion. However, this hypothesis was not entirely supported by the results of multivariate analysis assessing the independent positive correlations of each metabolite of each module with serum creatinine, serum bilirubin, and HE grade. Indeed, we found that 69% of metabolites were independently correlated with deterioration of the function of 2 (50% of metabolites) or 3 (19% of metabolites) organs, indicating the blood metabolite accumulation was a result of several independent mechanisms. Moreover, the mechanisms of blood metabolite accumulation in patients with ACLF and kidney failure may be complex. In these patients, blood metabolite accumulation may be a result of both renal hypofiltration and increased metabolite production by renal cells.<sup>20</sup> Of note, the multivariate analyses also showed that changes in the blood metabolome were more closely associated with deterioration of kidney or liver functions than with deterioration of brain function.

Our results strongly suggested a model in which changes in blood metabolites, in particular amino acids, may be best explained by a “metabolic reprogramming” whose primary purpose, as discussed below, was to fuel the intense systemic inflammatory response.

An important finding was that a single module (the yellow one) contained exclusively amino acids and the blood levels of most of these amino acids were increased in ACLF compared to AD. In the context of acute systemic inflammation, the activation of the hypothalamic-pituitary-adrenal axis results in glucocorticoid release that causes muscle proteolysis<sup>29</sup> and mobilization of amino acids.<sup>11,13,29</sup> Accordingly, the fact that the yellow-module membership exclusively included amino acids may be explained, at least in part, by their orchestrated mobilization from skeletal muscles.

In ACLF, activated innate immune responses included, for example, stimulation of bone marrow myelopoiesis (a proliferative process) resulting in peripheral-blood leukocytosis; activation of innate immune cells to produce a myriad of inflammatory molecules; and stimulation of hepatocytes to produce a broad variety of acute-phase proteins involved in the innate immune response.<sup>1,2</sup> Execution of these immune responses is known to rely on anabolic, energy-consuming, cell-intrinsic metabolic pathways involved in *de novo* synthesis of molecules including nonessential amino acids, purine and pyrimidine nucleotides, and ultimately proteins.<sup>11,12</sup> In innate immune cells, stimulation of PAMP receptors<sup>30</sup> or of cytokine receptors<sup>30</sup> transduce signals that activate glycolysis and *de novo* nucleotide synthesis<sup>15,31</sup> (Fig. S17A-C). In our study, 70% of the yellow-module amino acid members were proteinogenic amino acids, *i.e.* amino acids that can be incorporated into proteins under mRNA direction. Therefore, their mobilization from skeletal muscle in ACLF, was probably explained by the necessity to

fuel *de novo* protein synthesis in cells involved in the innate immune response. Moreover, features of increased glycolysis (and PPP), extraction of Krebs cycle intermediates and nucleotide synthesis, found in blood from patients with ACLF may also be explained by the necessity to fuel immune activation.

Ketone bodies can be produced from the hepatic catabolism of fatty acids and of 6 amino acids<sup>13</sup> (Fig. S15A). In acute systemic inflammation, including ACLF, the hepatic production of ketone bodies relies on catabolism of ketogenic amino acids because of the inhibition of fatty acid oxidation, which was witnessed by blood accumulation of acylcarnitines.<sup>10,13</sup> In our study, 5 ketogenic amino acids were in the yellow module, and we found features indicating their enhanced catabolism in ACLF (Figs. S15B, S16; Table 1). However, despite this extensive catabolism,  $\beta$ -hydroxybutyrate was not detectable in our patients, suggesting a defect or an inhibition of ketogenesis from amino acids. If this was the case, patients with ACLF might benefit from  $\beta$ -hydroxybutyrate administration because of the protective effects of this ketone body.

Our study provided other interesting results. In ACLF, we identified features suggesting the activation of the transsulfuration pathway which is a branch of the methionine cycle (a component of one-carbon metabolism network).<sup>16</sup> Because the transsulfuration pathway gives rise to the antioxidant glutathione (Fig. 5), activation of this pathway makes sense in ACLF where systemic oxidative stress occurred, as indicated by increased HNA2 levels.<sup>2</sup>

This study showed that the blood levels of the polyamine spermidine, which is a product of methionine and ornithine metabolism, were decreased in ACLF; this may be explained by polyamine skewing towards GABA synthesis. Because spermidine is an inducer of autophagy,<sup>17</sup> a decrease in spermidine may play a role in the decrease in autophagy recently found in ACLF.<sup>32</sup> Collectively, these findings may have potential therapeutic consequences (supplementary discussion). Several other questions regarding changes in amino acid metabolism found in patients with ACLF, in particular those related to methionine metabolism, tryptophan catabolism, urea cycle, and the potential impact of metabolic costs of immunity on peripheral-organ functions, need to be addressed in future studies (supplementary discussion).

Our study has limitations because of its descriptive design. Indeed, our hypotheses were not challenged by mechanistic investigations in animal models and we did not explore the blood metabolome in patients with acute systemic inflammation (*e.g.* sepsis) without cirrhosis. Nevertheless, analysis of the literature indicated that certain blood metabolic alterations were shared by patients without cirrhosis who had sepsis and poor outcome and our patients with ACLF. Indeed, like our patients with ACLF relative to those with AD, patients without cirrhosis who died from sepsis had higher baseline blood levels of pyruvate, lactate,  $\alpha$ -ketoglutarate, oxaloacetate, and acylcarnitines than those who survived.<sup>23</sup> However, unlike patients without cirrhosis who had sepsis,<sup>23</sup> our patients did not have blood accumulation of ketone bodies, suggesting that this lack of accumulation may be a hallmark of ACLF. Moreover, to our knowledge, the present study is the first to show in a large series of patients with acute systemic inflammation, the existence of multiple alterations in the one-carbon metabolism network, a decrease in spermidine levels and a possible connection with GABA synthesis.

In conclusion, our results suggest that, in ACLF, amino acids may be mobilized from skeletal muscles or derived from Krebs cycle intermediates to fuel anabolic programs, including protein and nucleotide synthesis. Ketogenic amino acids were extensively catabolized to produce energy substrates in peripheral organs, an effect that was insufficient because organs failed. Finally, blood levels of the polyamine spermidine, which is a potent inducer of autophagy and has anti-inflammatory effects, were decreased in ACLF. Future studies should investigate whether modifications of nutritional support could be used to reduce systemic inflammation and improve organ function.

### Abbreviations

ACLF, acute-on-chronic liver failure; AD, acute decompensation without ACLF; DAMPs, damage-associated molecular patterns; HE, hepatic encephalopathy; HNA2, human nonmercaptalbumin-2; IL-, interleukin-; INR, international normalized ratio; MTA, 5'-deoxy-5'-(methylthio)adenosine; PAMPs, pathogen-associated molecular patterns; PPP, pentose phosphate pathway; WGCNA, weighted gene co-expression network analysis.

### Financial support

The study was supported by the European Foundation for the Study of Chronic Liver Failure (EF-Clif). The EF-Clif is a non-profit private organization. Emmanuel Weiss is an EF-Clif Visiting Professor. The EF-Clif receives unrestricted donations from Cellex Foundation and Grifols, and is partner or contributor in several EU Horizon 2020 program projects. The funders had no influence on study design, data collection and analysis, decision to publish or preparation of the manuscript.

### Conflicts of interest

Dr. Janan has research collaborations with Yaqrit and Takeda. Dr. Janan is the inventor of OPA, which has been patented by UCL and licensed to Mallinckrodt Pharma. He is also the founder of Yaqrit limited, a spin out company from University College London and Thoreris Ltd. Dr. Bernardi is part of the speakers' bureau for Grifols SA, Octapharma AG, Shire/Takeda, CLS Behring GmbH, and PPTA, and is a consultant for Grifols SA, CLS Behring GmbH, Martin Pharmaceuticals and Shire/Takeda.

The remaining authors disclose no conflicts.

Please refer to the accompanying ICMJE disclosure forms for further details.

### Authors' contributions

Study concept and design (RM, VA); acquisition of clinical data and samples (GZ, PC, MB, PA, RJ); bioinformatic and statistical analyses (FA, JLL, AC, FF, FC, CJ); acquisition of metabolomic data (FF, FC, CJ), integration of clinical and biological results and interpretation of data (GZ, FA, JLL, AC, JC, RM); drafting of the manuscript (RM, VA); critical revision of the manuscript for important intellectual content (GZ, FA, PC, JC, FF, CJ, CF, EW, MB, PA, RJ); study supervision (RM, VA).

### Data availability statement

The metabolomic data set used in this study is available in J Hepatol 2020;72:688-701.

### Supplementary data

Supplementary data to this article can be found online at <https://doi.org/10.1016/j.jhep.2020.11.035>.

## References

Author names in bold designate shared co-first authorship

- [1] Moreau R, Jalan R, Ginès P, Pavesi M, Angeli P, Cordoba J, et al. Acute-on-chronic liver failure is a distinct syndrome that develops in patients with acute decompensation of cirrhosis. *Gastroenterology* 2013;144:1426-1437. 1437.
- [2] **Clària J, Stauber RE**, Coenraad MJ, Moreau R, Jalan R, Pavesi M, et al. Systemic inflammation in decompensated cirrhosis. Characterization and role in acute-on-chronic liver failure. *Hepatology* 2016;64:1249-1264.
- [3] Trebicka J, Fernández J, Papp M, Caraceni P, Laleman W, Gambino C, et al. The PREDICT study uncovers three clinical courses of acutely decompensated cirrhosis that have distinct pathophysiology. *J Hepatol* 2020;73:842-854.
- [4] Bajaj JS, O'Leary JG, Reddy KR, Wong F, Biggins SW, Patton H, et al. Survival in infection-related acute-on-chronic liver failure is defined by extrahepatic organ failures. *Hepatology* 2014;60:250-256.
- [5] Arroyo V, Moreau R, Jalan R. Acute-on-chronic liver failure. *N Engl J Med* 2020;382:2137-2145.
- [6] Arroyo V, Moreau R, Kamath PS, Jalan R, Ginès P, Nevens F, et al. Acute-on-chronic liver failure in cirrhosis. *Nat Rev Dis Prim* 2016;2:16041.
- [7] Moreau R, Elkrief L, Bureau C, Perarnau JM, Thévenot T, Saliba F, et al. Effects of long-term norfloxacin therapy in patients with advanced cirrhosis. *Gastroenterology* 2018;155. 1816-1827.e9.
- [8] Jansen C, Chatterjee DA, Thomsen KL, Al-Kassou B, Sawhney R, Jones H, et al. Significant reduction in heart rate variability is a feature of acute decompensation of cirrhosis and predicts 90-day mortality. *Aliment Pharmacol Ther* 2019;50:568-579.
- [9] **Praktiknjo M, Monteiro S**, Grandt J, Kimer N, Madsen JL, Werge MP, et al. Cardiodynamic state is associated with systemic inflammation and fatal acute-on-chronic liver failure. *Liver Int* 2020;40:1457-1466.
- [10] **Moreau R, Clària J, Aguilar F, Fenaille F**, Lozano JJ, Junot C, et al. Blood metabolomics uncovers inflammation-associated mitochondrial dysfunction as a potential mechanism underlying ACLF. *J Hepatol* 2020;72:688-701.
- [11] **Wang A, Luan HH**, Medzhitov R. An evolutionary perspective on immunometabolism. *Science* 2019;363(6423). eaar3932.
- [12] Ganeshan K, Chawla A. Metabolic regulation of immune responses. *Annu Rev Immunol* 2014;32:609-634.
- [13] **Ganeshan K, Nikkanen J, Man K, Leong YA**, Sogawa Y, Maschek JA, et al. Energetic trade-offs and hypometabolic states promote disease tolerance. *Cell* 2019;177. 399-413.e12.
- [14] Pareek V, Tian H, Winograd N, Benkovic SJ. Metabolomics and mass spectrometry imaging reveal channelled de novo purine synthesis in cells. *Science* 2020;368(6488):283-290.
- [15] **Villa E, Ali ES, Sahu U**, Ben-Sahra I. Cancer cells tune the signaling pathways to empower de novo synthesis of nucleotides. *Cancers (Basel)* 2019;11. pii: E688.
- [16] Sanderson SM, Gao X, Dai Z, Locasale JW. Methionine metabolism in health and cancer: a nexus of diet and precision medicine. *Nat Rev Canc* 2019;19:625-637.
- [17] **Madeo F, Eisenberg T**, Pietroccola F, Kroemer G. Spermidine in health and disease. *Science* 2018;359(6374). pii: eaan2788.
- [18] Vander Heiden MG, DeBerardinis RJ. Understanding the intersections between metabolism and cancer biology. *Cell* 2017;168:657-669.
- [19] Kanarek N, Petrova B, Sabatini DM. Dietary modifications for enhanced cancer therapy. *Nature* 2020;579:507-517.
- [20] **Clària J, Moreau R**, Fenaille F, Amorós A, Junot C, Gronbaek H, et al. Orchestration of Tryptophan-Kynurenine pathway, acute decompensation and acute-on-chronic liver failure in cirrhosis. *Hepatology* 2019;1686-1701.
- [21] Praktiknjo M, Clees C, Pigliacelli A, Fischer S, Jansen C, Lehmann J, et al. Sarcopenia is associated with development of acute-on-chronic liver failure in decompensated liver cirrhosis receiving transjugular intrahepatic portosystemic shunt. *Clin Transl Gastroenterol* 2019;10: e00025.
- [22] **Praktiknjo M, Book M**, Luetkens J, Pohlmann A, Meyer C, Thomas D, et al. Fat-free muscle mass in magnetic resonance imaging predicts acute-on-chronic liver failure and survival in decompensated cirrhosis. *Hepatology* 2018;67:1014-1026.
- [23] **Langley RJ, Tsalik EL, van Velkinburgh JC**, Glickman SW, Rice BJ, Wang C, et al. An integrated clinico-metabolomic model improves prediction of death in sepsis. *Sci Transl Med* 2013;5:195ra95.

- [24] Gao X, **Sanderson SM**, **Dai Z**, Reid MA, Cooper DE, Lu M, et al. Dietary methionine influences therapy in mouse cancer models and alters human metabolism. *Nature* 2019;572:397–401.
- [25] Langfelder P, Horvath S. WGCNA: an R package for weighted correlation network analysis. *BMC Bioinformatics* 2008;9:559.
- [26] Pei G, Chen L, Zhang W. WGCNA application to proteomic and metabolomic data analysis. *Methods Enzymol* 2017;585: 135–158.9.
- [27] Scott Chialvo CH, Che R, Reif D, Reed LK. Eigenvector metabolite analysis reveals dietary effects on the association among metabolite correlation patterns, gene expression, and phenotypes. *Metabolomics* 2016;12. pii:167.
- [28] Hernandez-Rabaza V, Cabrera-Pastor A, Taoro-Gonzalez L, Gonzalez-Usano A, Agusti A, Balzano T, et al. Neuroinflammation increases GABAergic tone and impairs cognitive and motor function in hyperammonemia by increasing GAT-3 membrane expression. Reversal by sulforaphane by promoting M2 polarization of microglia. *J Neuroinflammation* 2016;13:83.
- [29] Bodine SC, Latres E, Baumhueter S, Lai VK, Nunez L, Clarke BA, et al. Identification of ubiquitin ligases required for skeletal muscle atrophy. *Science* 2001;294:1704–1708.
- [30] Koyasu S. The role of PI3K in immune cells. *Nat Immunol* 2003 Apr;4:313–319.
- [31] Saxton RA, Sabatini DM. mTOR signaling in growth, metabolism, and disease. *Cell* 2017;168:960–976.
- [32] **Wan J**, **Weiss E**, **Ben Mkaddem S**, Mabire M, Choinier PM, Thibault-Sogorb T, et al. LC3-associated phagocytosis protects against inflammation and liver fibrosis via immunoreceptor inhibitory signaling. *Sci Transl Med* 2020;12(539):eaaw8523.